THE CHANGE OF THE LOCAL CRACK DRIVING FORCE IN AN UNDER-MATCH WELDED JOINT

Jožef Predan[1], Nenad Gubeljak[1], Otmar Kolednik[2], F.D. Fischer[3]

[1] University of Maribor, Faculty of Mechanical Engineering
Smetanova 17, Maribor, Slovenia
email: jozef.predan@uni-mb.si
[2] Erich Schmid Institute of Materials Science, Austrian Academy of Sciences
Jahnstrasse 12, A-8700 Leoben, Austria
email: kolednik@unileoben.ac.at
[3] Institute of Mechanics, Montanuniversität Leoben and Erich Schmid Institute
Franz-Josef Strasse 13, A-8700 Leoben, Austria
email: mechanik@unileoben.ac.at

Abstract

The crack growth resistance of an inhomogeneous welded joint, produced by a Flux Cord Arc Welding procedure is measured in terms of the crack tip opening displacement δ_5. The crack grows from the under-matched weld metal with a lower yield strength and a higher Young's modulus through an interface into the over-matched weld metal with higher yield strength and lower Young's modulus. The test is simulated by a 2D finite element analysis. The crack extension is controlled so that the computed δ_5 vs. load curve matches as good as possible the experimental curve. The local differences in the mechanical properties induce an additional crack driving force term, the material inhomogeneity term C_{inh}. The magnitude of C_{inh} is evaluated by a post-processing procedure. The computations show that C_{inh} is negative and diminishes the effective crack driving force appreciably, especially when the crack tip is close to the interface.

Introduction

It is known long since that the effective, near-tip crack driving force (CDF) J_{tip} becomes different from the nominally applied far-field CDF J_{far}, if the material properties vary in the direction of the crack extension. Simha et. al. [1,2] have developed a model, based on the Eshelby material forces approach, to quantify the effect for arbitrary constitutive relations of the materials. Continuous variations of the material properties have been treated [1], as well as discrete jumps of the material properties at a sharp interface [2,3]. It is seen from the model that the material inhomogeneity induces an additional CDF-term, called the material inhomogeneity term C_{inh} which leads to a shielding or anti-shielding of the crack tip. So far, the model has been applied exemplarily to Compact Tension bimaterial specimens with a stationary crack. It has been shown that C_{inh} is positive and enhances the effective near-tip CDF, if the crack is located in the material with the higher yield strength or the higher elastic modulus (hard/soft or stiff/compliant transition), and vice versa.

The purpose of this paper is to apply the theory to a welded joint with a strength mis-match interface and to evaluate C_{inh} for both a stationary and a propagating crack. It should be noted that a strength mis-match welded joint exhibits locally different microstructures causing local variations of the Young's modulus, the yield strength, and the strain hardening

exponent. The assessment of the material inhomogeneity term is, therefore, essential to understand the fracture resistance of the welded joint. A long-term goal would be to take into account the material inhomogeneity into the structural-integrity assessment procedure, e.g., SINTAP [4].

Materials and welding

A 30 mm thick high-strength low-alloy HSLA steel plate (grade HT 50) was welded using a Flux Cord Arc Welding (FCAW) process. Two different tubular wires were selected for the welding in order to produce welded joints in over- and under-matched (OM and UM) configurations. The chemical compositions and mechanical properties of the base metal (BM) and the OM and UM weld metals are listed in Tables 1 and 2, respectively.

TABLE 1. Chemical composition of base metal and consumables in weight percentages.

Material	C	Si	Mn	P	S	Cr	Mo	Ni
OM weld metal	0.040	0.16	0.95	0.011	0.021	0.49	0.42	2.06
Base metal	0.123	0.33	0.56	0.003	0.002	0.57	0.34	0.13
UM weld metal	0.096	0.58	1.24	0.013	0.160	0.07	0.02	0.03

TABLE 2. Mechanical properties of base metal and consumable.

Material	E [GPa]	$R_{p0.2}$ [MPa]	R_m [MPa]	σ_y [MPa]	n [1]	$M = R_{p0.2,WM} / R_{p0.2,BM}$
OM weld metal	184	648	744	616	0,085	1,19
Base metal	203	545	648	516	0,089	-
UM weld metal	208	469	590	436	0,105	0,86

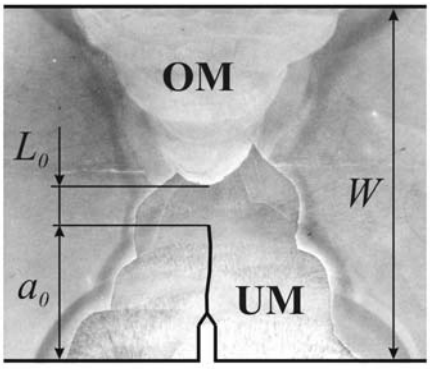

FIGURE 1. Cross-section of the welded joint with notch position in UM weld metal.

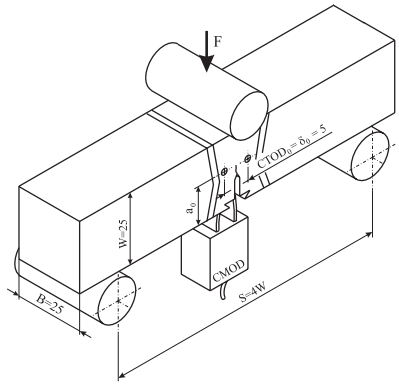

FIGURE 2. Specimen geometry and configuration for CTOD testing.

The strength mis-match factors *M*, i.e., the ratio between the technical yield stress $R_{p0.2}$ of the weld metal to those of the BM, are also given in Tab. 2. The values of the physical yield stress σ_y and the strain hardening exponent *n*, which are needed for the numerical analysis, are also listed. Figure 1 shows a cross section of the inhomogeneous multi-pass weld joint with half OM- and half UM weld metal. The described welding procedure is usually used for repair welding or for welded joints where possibly cold hydrogen assisted cracking can appear.

CTOD testing

Fracture mechanics tests were performed to determine the fracture behavior of the considered welded joints. The crack growth resistance was measured in terms of the crack tip opening displacement (CTOD), analyzed both according to the Standard BS 7448 [5] and the GKSS δ_5 testing procedure[6]. Hereby, δ_5 is measured over a gauge length of 5 mm at the specimen side surfaces at the position of the tip of the fatigue pre-crack. Figure 2 shows the geometry of the single edge notch bend (SENB) specimen and the testing configuration. The fatigue pre-crack is located in UM weld metal at a distance of L=0.76 mm before the interface, i.e., the fusion line between UM and OM weld metals. The CTOD tests were performed at room temperature (+24°C) under displacement control at a loading rate of 1 mm/min. The load *F*, the load point displacement, the crack mouth opening displacement (CMOD), and δ_5 were recorded during the tests. Figure 3 shows the δ_5 vs. *F* plot. After a certain amount of stable crack growth in the UM metal, a small step of unstable crack propagation is noticed shortly after the maximum load. The crack propagates stably into the OM metal. As the crack grows from the UM to the OM weld metal (a transition soft/hard) and as the difference in the elastic modulus is relatively small, we expect a negative value of the material inhomogeneity term C_{inh} and a reduction of the effective CDF, compared to the far-field CDF.

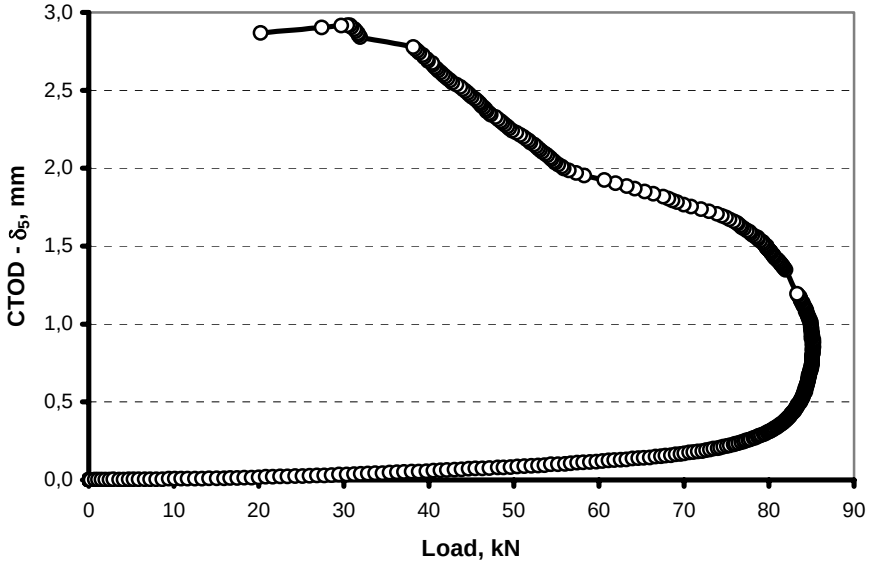

FIGURE 3. Experimentally obtained δ_5 vs. load curve.

Numerical modeling

For the numerical analyses, we use a commercial implementation (ABAQUS Version 6.4) of a finite-element method (FEM). The SENB specimen has an initial crack length of $a_0 = 7.11$ mm and a distance between crack tip and fusion line of $L_0 = 0.76$ mm. Figure 4 shows the mesh in the region around the crack tip. The elastic-plastic materials are modelled using an incremental plasticity model provided by ABAQUS. The loading is performed by prescribing the experimentally obtained load-point displacement. δ_5 is determined as the displacement at the node 2.5 mm distant from the crack plane at the height of the fatigue pre-crack tip.

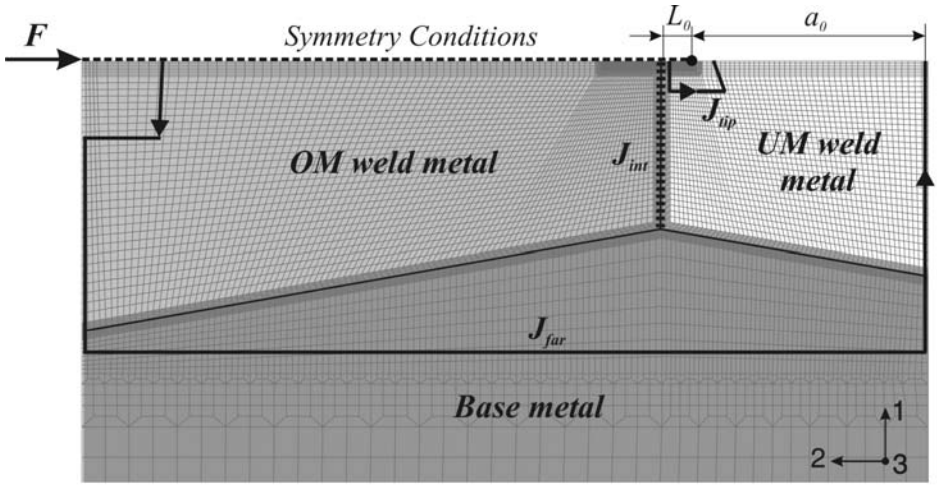

FIGURE 4. The material configuration in the SENB specimen with an interface perpendicular to the crack plane, with FEM mesh and *J*-integral paths.

After each increment of displacement, the equilibrium stress and strain fields are computed. Subsequently, the material inhomogeneity term, C_{inh}, can be calculated by a post-processing procedure as [2,3]

$$C_{inh} = -\int_{\Sigma} \left([\![\phi]\!] - \langle \sigma_{ik} \rangle [\![\varepsilon_{ik}]\!] \right) n_j \, e_j \, ds = -J_{\text{int}} . \quad (1)$$

$[[\phi]]$ denotes the jump of the strain energy density, $[[\varepsilon_{ik}]]$ the jump of the strain tensor, and $\langle \sigma_{ik} \rangle$ the mean value of the local stress tensor on both sides of the interface Σ. The normal vector to the interface and the crack growth direction are designated as n_j and e_j, respectively. It has been demonstrated in [2] that C_{inh} can be also evaluated by calculating the J-integral around the interface, J_{int}. This value and the values of J_{tip} and J_{far} are evaluated using the virtual crack extension method of ABAQUS. For a stationary crack, the condition

$$J_{tip} = J_{far} + C_{inh} \quad (2)$$

is fulfilled. But this condition does not hold for a growing crack as then *J* becomes path dependent even for a homogeneous material. The paths for evaluating the J-values are indicated in Fig. 5. It should be noted that it is often difficult to evaluate accurately the effective near-tip J-integral, J_{tip}.

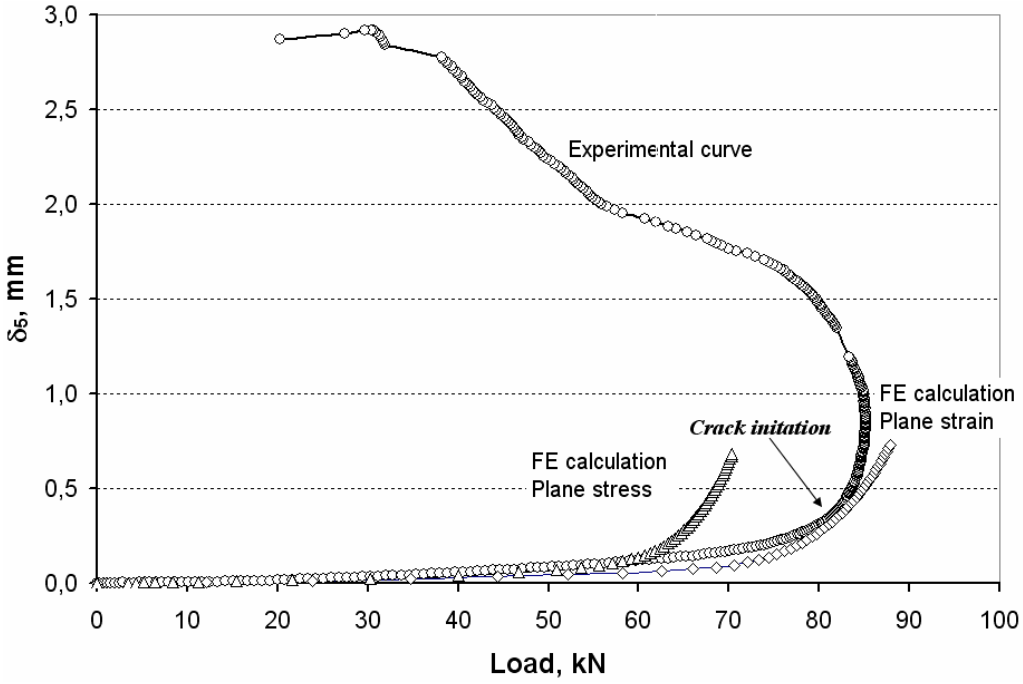

FIGURE 5. Results of the 2D plane stress and plane strain FE computations for a stationary crack in comparison to the experimentally measured curve.

Figure 5 shows the computed δ_5 vs. F curves for plane stress and plane strain conditions for a stationary crack together with the experimental δ_5 vs. F curve. The point of initiation of stable crack growth is also indicated. A realistic 3D simulation of crack growth would be

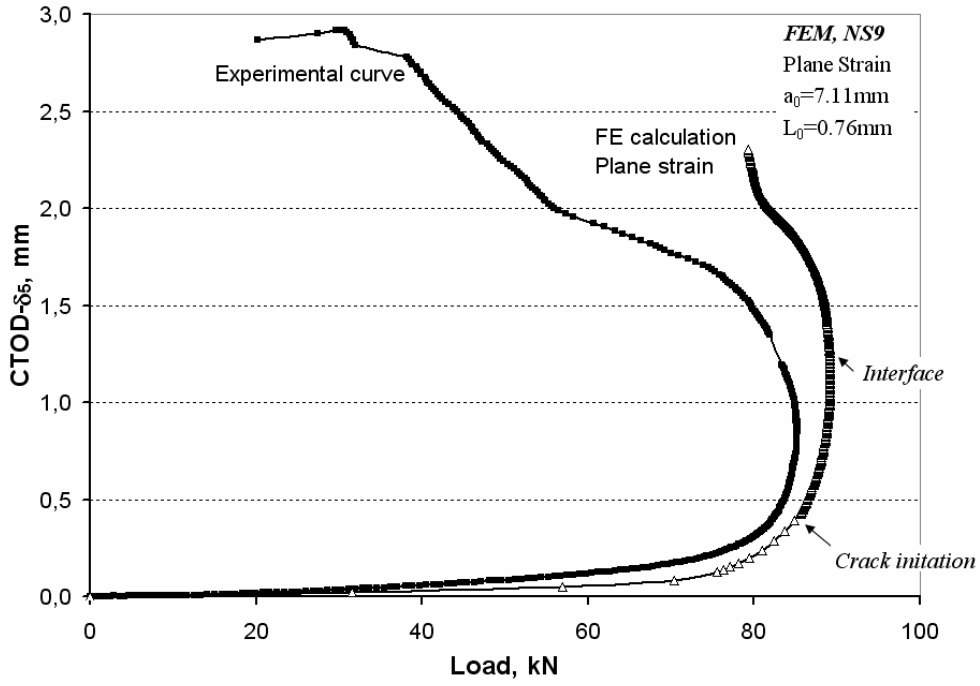

FIGURE 6. Comparison between 2D plane strain FEM result with crack growth and the experimentally measured curve.

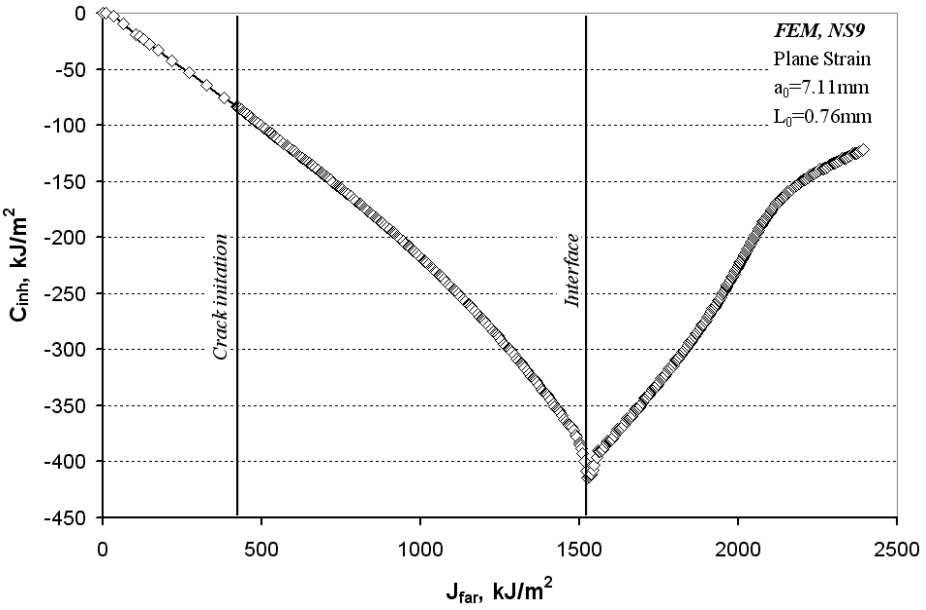

FIGURE 7. Material gradient term, $C_{inh} = J_{int}$, vs. far-field J-integral, J_{far}.

beyond the possibilities of this study; therefore, a 2D plane strain FEM computation was conducted, applying the node release technique. Herby, the crack extension is controlled so that the computed δ_5 vs. F curve matches as good as possible the experimental curve. Figure 6 compares the computed and experimental δ_5 vs. F curves.

Figure 7 shows the variation of the material gradient term during the crack extension: the material gradient term C_{inh} is plotted against the far-field crack driving force J_{far}.

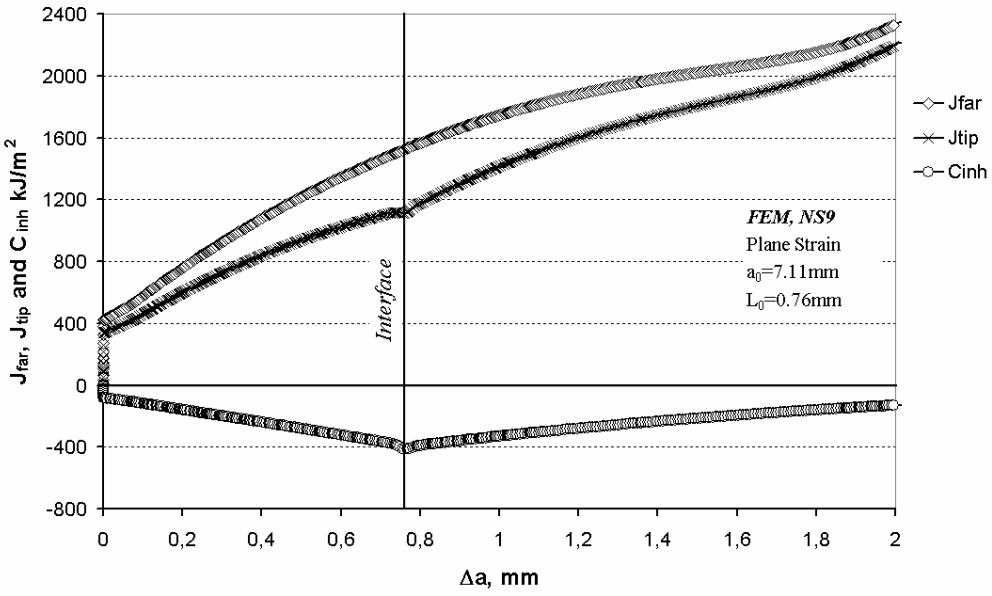

FIGURE 8. The change of the crack driving force during crack propagation through the fusion line of a strength mis-match welded joint.

Figure 8 shows the variations of J_{far}, C_{inh}, and the effective CDF J_{tip} during the crack extension Δa. The initiation of stable crack growth and the point where the crack reaches the interface are indicated. At very small loads C_{inh} is positive. This is caused by the slightly higher Young's modulus of the UM material (stiff/compliant transition), see Tab. 2. At these low loads, the effect of the yield strength inhomogeneity (soft/hard transition) is negligible as the plastic zone does not yet interfere with the interface [7,8]. At higher loading, the soft/hard transition of the yield strength has a much larger effect than the stiff/compliant transition of the elastic modulus, and C_{inh} becomes negative which means that it reduces the CDF (Eq. 2). When the crack reaches the interface C_{inh} amounts *–420* kJ/m^2; it reduces the effective CDF by more than 25%. Subsequently, for the growth in the OM material, C_{inh} reduces its size.

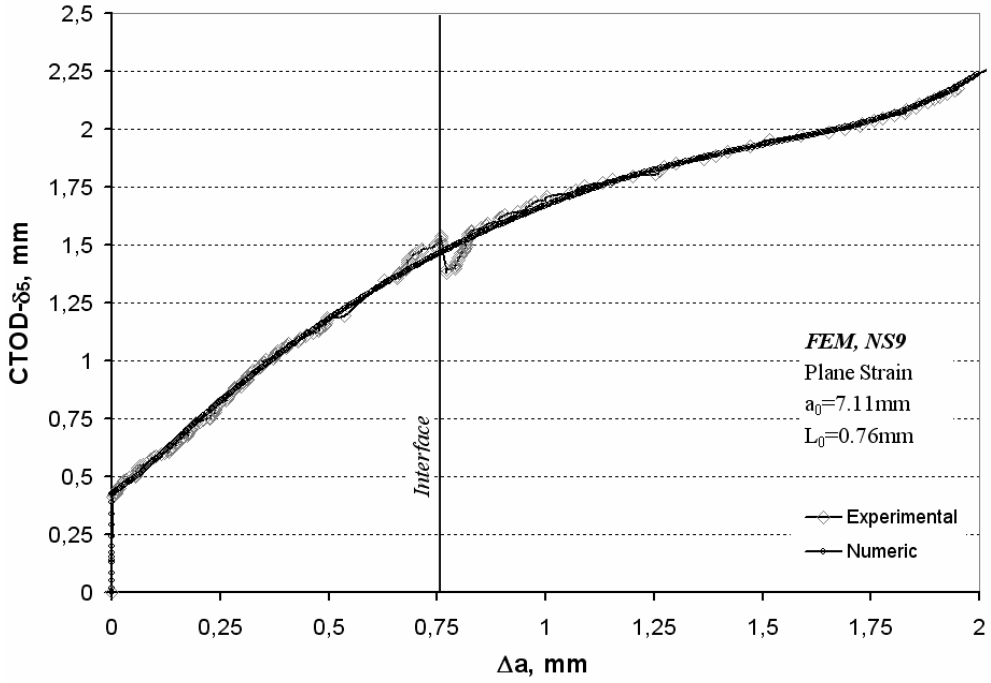

FIGURE 9. Comparison between computed and experimentally measured δ5 vs. crack extension curve.

In Figure 9, the computed δ_5 vs. Δa curve is compared to the experimentally measured curve. The curves are quite similar, in spite of the fact that the numerical analysis, being 2D, does not model the actual behaviour of the specimen, but gives a through-thickness average of the plasticity with increasing crack extension.

Conclusion

A Flux Cord Arc Welding procedure was applied to produce an inhomogeneous welded joint. On 3-point bend specimens, crack growth resistance curves were determined in terms of the crack tip opening displacement δ_5. The global mechanical properties of the base metal, the two weld metals, and the heat affected zone are determined by tests on miniaturized tensile specimens. The crack tip was located in the UM weld metal with the lower yield strength and the higher Young's modulus and the crack grew through an interface into the OM weld metal

with higher yield strength and lower Young's modulus. The test was simulated by a 2D finite element analysis for plane strain conditions. The crack extension was controlled so that the computed δ_5 vs. load curve matches as good as possible the experimental curve. The local differences in the mechanical properties induce an additional crack driving force term, called the material inhomogeneity term, C_{inh}. The magnitude of C_{inh} was evaluated by a post-processing procedure based on the material forces approach. The computations have shown that C_{inh} is negative and diminishes the effective crack driving force appreciably, especially when the crack tip is close to the interface.

Acknowledgments

The authors want to thank the GKSS Research Center Geesthacht, Germany for the support in CTOD testing and Dr. G.X. Shan, VOEST Alpine Industrieanlagenbau GmbH&Co, Linz, Austria for the support in the FEM calculations. The authors acknowledge the financial support by the Österreichischer Austauschdienst (ÖAD) and the Slovenian Ministry of Education, Science and Sport within the frame of the bilateral project Sl-A12/0405, and by the Materials Center Leoben under the project number SP14.

References

1. Simha, N.K., Fischer, F. D., Kolednik, O. and Chen, C. R., *J. Mech. Phys. Solids*, vol. 51, 209-240, 2003.
2. Simha, N.K., Predan, J., Kolednik, O., Fischer, F. D., and Shan, G.X., *J. Mech. Phys. Solids*, submitted.
3. Kolednik, O., Predan, J., Shan, G.X., Simha, N.K. and Fischer, F. D., *Int. J. Solids Struct*, in press.
4. SINTAP: Structural Integrity Assessment Procedure. Final Revision. EU-Project BE 95-1462. Brite Euram Programme, 1999.
5. *BS 7448: Fracture Mechanics Toughness Tests*, Part 2, British Standards Institution, London, 1997.
6. GKSS-Forschungszentrum Geesthacht: GKSS-Displacement Gauge Systems for Application in Fracture Mechanics, 1991.
7. Kolednik, O., *Int. J. Solids Struct*, vol. 37, 781-808, 2000.
8. Kolednik, O., Predan, J., Shan, G.X., Simha, N.K. and Fischer, F. D., In *Proceedings of the15th European Conference of Fracture*, submitted.